



Comprehensive study of the dynamic interaction between SO₂ and acetaldehyde during alcoholic fermentation

Thomas Ochando, Jean-Roch Mouret, Anne Humbert-Goffard, Evelyne Aguera, Jean-Marie Sablayrolles, Vincent Farines

► To cite this version:

Thomas Ochando, Jean-Roch Mouret, Anne Humbert-Goffard, Evelyne Aguera, Jean-Marie Sablayrolles, et al.. Comprehensive study of the dynamic interaction between SO₂ and acetaldehyde during alcoholic fermentation. Food Research International, 2020, 136, pp.109607. 10.1016/j.foodres.2020.109607 . hal-02941406

HAL Id: hal-02941406

<https://hal.inrae.fr/hal-02941406>

Submitted on 22 Aug 2022

HAL is a multi-disciplinary open access archive for the deposit and dissemination of scientific research documents, whether they are published or not. The documents may come from teaching and research institutions in France or abroad, or from public or private research centers.

L'archive ouverte pluridisciplinaire **HAL**, est destinée au dépôt et à la diffusion de documents scientifiques de niveau recherche, publiés ou non, émanant des établissements d'enseignement et de recherche français ou étrangers, des laboratoires publics ou privés.



Distributed under a Creative Commons Attribution - NonCommercial 4.0 International License

Comprehensive study of the dynamic interaction between SO₂ and acetaldehyde during alcoholic fermentation

Thomas OCHANDO^{1,2}, Jean-Roch MOURET¹, Anne HUMBERT-GOFFARD², Evelyne AGUERA³, Jean-Marie SABLAYROLLES¹, Vincent FARINES¹

¹SPO, INRAE, Univ Montpellier, Montpellier SupAgro, Montpellier, France

²Moët & Chandon, Epernay, France

³Pech Rouge, INRAE, Gruissan, France

*Corresponding author: Tel.: +33-4-99-61-22-74; Fax: +33-4-99-61-28-51

E-mail address: vincent.farines@inrae.fr

Abstract

In this work, we focused on the effect of the initial content of SO₂ in synthetic grape juice on yeast metabolism linked to the production of acetaldehyde. Lengthening of the lag phase duration was observed with an increase in the initial SO₂ content. Nevertheless, an interesting finding was a threshold value of an initial SO₂ content of 30 mg L⁻¹ in the juice led to equilibrium between intracellular SO₂ diffusion and SO₂ production from the sulfate pool by yeast. The ratios of free and bound acetaldehydes were measured during fermentation, and the maximum accumulation of free acetaldehyde was observed when SO₂ concentration equilibrium between diffusion and production was reached in the fermenting juice. Moreover, it was observed that SO₂ addition resulted in significant changes in the synthesis of aroma compounds. Production of volatile molecules related to sulfur metabolism (methionol) was changed. But, more surprisingly, synthesis of some volatile carbon compounds (diacetyl, isoamyl alcohol, isobutyl alcohol, phenyl ethanol and their corresponding esters) was also altered because of major disruptions in the NADPH/NADP⁺ redox equilibrium. Finally, we demonstrated that acetaldehyde bound to SO₂ could not be metabolized by the yeast during the time course of fermentation and that only free acetaldehyde could impact metabolism.

Keywords:

Acetaldehyde; sulfite; α-acetolactate; aromas; winemaking alcoholic fermentation

1. Introduction

In enology, sulfur dioxide (SO_2) is a major food additive used for its various beneficial effects, including antimicrobial effects, antioxidant properties and its impact on the color of wines (Blouin, 2014). Sulfur dioxide is a gas at room temperature and readily dissolves in liquids. Once dissolved into the aqueous form, sulfur dioxide acts as a diprotic acid ($\text{pK}_1 = 1.81$ and $\text{pK}_2 = 6.91$ at 20°C in H_2O) and dissociates into three fractions: molecular SO_2 ($\text{SO}_2 \cdot \text{H}_2\text{O}$), bisulfite (HSO_3^-) and sulfite (SO_3^{2-}), where pH and thermodynamic constants modulate the proportions of the different forms. In general, the pH of musts and wines varies between 3 and 4, and the dominant species are therefore bisulfite anions, with only a small amount of molecular SO_2 . Additionally, the antimicrobial effectiveness of SO_2 is mostly related to the amount of molecular SO_2 present, which is 500 times more active than bisulfite (Rehm & Wittmann, 1962), whereas bisulfite is the active antioxidant form. In a finished wine, the SO_2 content results not only from exogenous addition during the prefermentary operations (e.g., grape harvesting, pressing, settling) but also from synthesis during fermentation. Indeed, *Saccharomyces cerevisiae* can metabolize sulfate *via* the Sulfate Reduction Sequence (SRS) pathway. Inorganic sulfate is first taken up through a sulfate permease. Then, it is reduced to sulfide through a series of steps using the enzymes ATP-sulfurylase and sulfite reductase. The next step leads to the sequestering of the sulfide catalyzed by O-acetylserine/O-acetylhomoserine sulfhydrylases to respectively form cysteine and homocysteine which can then be converted to methionine (Swiegers et al., 2005). In the SRS pathway, the sulfate molecules reduction produces sulfite or sulfide which is partially excreted (Donalies & Stahl, 2002). Thus, wine yeasts are able to produce amounts of sulfites ranging from

a few mg L⁻¹ to more than 90 mg L⁻¹, depending on the fermentation conditions and the yeast strain (Eschenbruch & Bonish, 1976).

Once added to must or wine, a portion of the bisulfite form (HSO₃⁻) - also known as "bound SO₂" - will bind with compounds in the wine. Indeed, bisulfite is able to bind to many molecules, including carbonyl compounds, ketoacids, and sugars as well as a few others (Burroughs & Sparks, 1973). Acetaldehyde is the strongest HSO₃⁻ binder in fermenting musts and wines, forming adducts such as hydroxysulphonic acids. This combination generally represents the most significant portion of bound SO₂ in wine and is considered very strong, K_d: 10⁻⁶ M⁻¹ (Blouin, 2014). Even if the combination between SO₂ and acetaldehyde is very strong, it is important to note that acetaldehyde can also bind to polyphenols. Its combination to tannins forms acetaldehyde-bridged whose formation will change perception of astringency (Cheynier et al., 2006). It can also react with anthocyanins to form anthocyanin-derived pigments involved in wine color (Bakker & Timberlake, 1997).

From a metabolic point of view, acetaldehyde is formed from glycolysis which produces pyruvate as final product; pyruvate is then converted into acetaldehyde and CO₂ through pyruvate decarboxylase (PDC) enzymes. Acetaldehyde can be then transformed into ethanol by alcohol dehydrogenase (ADH) enzymes. This step is crucial for maintaining a redox balance in the cell, as it reoxidises NADH to NAD⁺, which is required for glycolysis (Pronk et al., 1996). More generally, acetaldehyde plays a key role in yeast metabolism as it is the precursor of different molecules: acetate (catalyzed by aldehyde dehydrogenase), acetoin (catalyzed by PDC) and α-acetolactic acid (catalyzed by acetolactate dehydrogenase enzymes) which is later converted into acetoin and 2,3-butanediol (Romano & Suzzi, 1996). Acetaldehyde is also the indirect precursor of volatile compounds responsible for aromas (isobutyl

alcohol, active amyl alcohol and isoamyl alcohol) through the synthesis of α -acetohydroxybutyrate (catalyzed by aldehyde dehydrogenase).

The production dynamics of acetaldehyde during alcoholic fermentation can be divided into 3 phases. Early formation was observed during the lag phase at the onset of fermentation before any detectable growth (Cheraiti et al., 2010). The initial level of sulfites in the must can affect the duration of the lag phase (Ferreira et al., 2017) due to the toxicity of sulfites to yeasts. One resistance mechanism against sulfur dioxide appeared to be the release of acetaldehyde by yeasts to bind HSO_3^- (Aranda et al., 2006). The accumulation of acetaldehyde continued during the growth phase, and the concentration decreased during the stationary phase until the end of alcoholic fermentation (Jackowetz et al., 2011). It was shown that (i) the residual amounts of acetaldehyde at the end of fermentation were independent of the quantities accumulated during fermentation (Cheraiti et al., 2010; Liu & Pilone, 2000) and that (ii) acetaldehyde production was higher in the presence of SO_2 (Herraiz et al., 1989; Jackowetz et al., 2011).

Finally, the differences between free and bound acetaldehyde production relative to initial sulfite levels or SO_2 dynamics during alcoholic fermentation were not discussed in any of these earlier studies.

The objective of the present article is to investigate the impact of SO_2 addition on the fermentation process and the production of aroma compounds linked to free acetaldehyde by using a new approach based on a precise monitoring – including online measurements – of the dynamics of synthesis or consumption of free and bound acetaldehyde and SO_2 . We thus focused on the evolution of free and bound SO_2 but also on the interaction between SO_2 and acetaldehyde to better understand

the mechanisms involved in the production of these two key compounds during alcoholic fermentation.

2. Materials and methods

2.1. Fermentations

All the fermentations were performed in triplicate with 10 L stainless steel fermenters equipped with gas mass flow meters (Bronkhorst, High-Tech BV, Ruurlo, Netherlands) for online measurement of CO₂ production rate (dCO₂/dt) and containing 9 L of synthetic grape juice at 20°C. Synthetic medium derived from standard grape juice (Bely et al., 1990) and contained notably 180 g L⁻¹ of sugars (half glucose and fructose). The assimilable nitrogen concentration was 360 mg N L⁻¹ with a mixture of ammonium (30%) and amino acids (70%). Concentrations of amino acids, acids (malic and tartaric), vitamins and trace elements were identical to those used in our previous studies (Ochando et al., 2016). The pH of the medium was 3.1. Fermentations were carried out with a *S. cerevisiae* strain isolated from the Champagne vineyard and property of the company Moët et Chandon (Epernay, France). This strain is available in our collection under the reference code MC005 and accessible upon request. Fermentation tanks were inoculated with 10 g hL⁻¹ active dry yeast that was previously rehydrated for 30 min at 30°C in a 50 g L⁻¹ glucose solution.

In some fermentations, various amounts (up to 7mM) of free acetaldehyde or sodium 1-hydroxyethanesulphonate (HES) were added at different time points of the stationary phase. Addition of acetaldehyde was carried out from a stock solution of commercial product (CAS: 75-07-0, ≥99.5%, Sigma-Aldrich®) whereas addition of HES was realized from the product synthesized in our laboratory.

2.2. Synthesis of sodium 1-hydroxyethanesulphonate

This product was directly synthesized by mixing sodium metabisulfite (CAS: 7681-57-4, $\geq 97.0\%$, Sigma-Aldrich®) with acetaldehyde (CAS 75-07-0, $\geq 99.5\%$, Sigma-Aldrich®) in excess to avoid the presence of free SO_2 at the end of synthesis. 3 g of acetaldehyde was incorporated in a graduated flask containing 60 mL of sodium metabisulfite solution (41.8 g L^{-1} i.e. $0.44 \text{ mol L}^{-1} \text{ SO}_2$), pH 4.3. At this pH, more than 99.4% of the SO_2 in solution is in the ionic form of HSO_3^- . Then, the flask was filled to 100 mL with the sodium metabisulfite solution and the reaction mixture was incubated at 37°C for 1 hour. Excess of acetaldehyde was eliminated with a vacuum rotary evaporator (Buchi SARL, Rungis, France) at 30°C for 15 min..

The synthesized product was analyzed by nuclear magnetic resonance (NMR) using an Agilent 500 MHz DD2 NMR spectrometer (Agilent Technologies, Santa Clara, CA, USA) equipped with a 5 mm indirect detection Z-gradient probe at 25°C in D_2O .

Trimethylsilylpropanoic acid (TSP) was used as the chemical shift standard. The NMR spectra (^1H , provided in the supplementary data) showed that the carbon compounds obtained were 1-hydroxyethanesulphonate ($\text{NaO}_3\text{S-CH(OH)-CH}_3$), sodium hydrate acetaldehyde (NaO-CH(OH)-CH_3) and some free acetaldehyde ($\text{CH}_3\text{-CHO}$). Accurate concentration determinations of the compounds were performed using VNMRJ-CRAFT software for peak deconvolution and the absolute intensity qNMR method with external calibration for molarity calculation from surface signal integration (Ferreira-Lima et al., 2016). From this analysis, a 351 mM concentration of 1-HES was obtained, with 14.4 mM sodium hydrate acetaldehyde acid and 13.3 mM free acetaldehyde. Acetaldehyde bound to sodium sulfite or HSO_3^- represented approximately 93% of the synthesis products. Free acetaldehyde

represented less than 4% of the total amount of acetaldehyde at the end of synthesis.

2.3. Determination of free and total SO₂

Iodometric titration (iodide / iodate oxidizing solution) was performed with an automatic double platinum electrode titration apparatus (Iodo 980, Dujardin Salleron, Narbonne, France) (Zoecklein et al., 1999). Potassium iodide (CAS: 7681-11-0, ≥99.0%), potassium iodate (CAS: 77581-05-6, ≥99.9%), sodium hydrogen carbonate (CAS: 144-55-8, ≥99.7%), sodium hydroxide (CAS: 1310-73-2, ≥98.0%) and sulfuric acid (CAS: 7664-93-9, ≥99.9%) were of analytical grade (Sigma-Aldrich®). For SO₂ titration, the volume of the I₂ (0.002 eq L⁻¹) burette drop was multiplied by 2.58 or 6.54 for direct expression of the amount in mg L⁻¹ of free and total SO₂ respectively.

2.4. Determination of free and total acetaldehyde

During the fermentation, the concentration of free acetaldehyde in the gas phase was analyzed using the online device described by Morakul (Morakul et al., 2011).

On the basis of the concentration of free acetaldehyde in the gas phase, the concentration of free acetaldehyde in the liquid was calculated using the partition coefficient $K_i (= C_{gas}/C_{liquid})$ estimated at any time of fermentation from the sugar content, ethanol content and temperature (Aguera et al., 2018):

$$K_i = \beta_0 \cdot T + \beta_1 \cdot T \cdot \exp(-\beta_2 \cdot [Ethanol]) + \beta_3 \cdot T \cdot \exp(-\beta_4 \cdot [Glucose]) + \varepsilon$$

where β_0 is the slope of the temperature effect; β_2 and β_4 are the coefficients corresponding to the effects of the ethanol and glucose concentrations, respectively; β_1 and β_3 are the coefficients corresponding to the effects of the interaction between

temperature and ethanol or glucose, respectively; and ϵ is an independent $N(0, \sigma^2)$ error term.

The total acetaldehyde content in the liquid was determined by enzymatic method with a Thermo Fisher Scientific® kit (Ref: 984347) and a Thermo Scientific™ Gallery™ Automated Photometric Analyser.

2.5. GC/MS analysis

The concentrations of higher alcohols and esters were measured in the liquid phase after pretreatment of the sample by double liquid-liquid extraction with dichloromethane in the presence of deuterated standards (Rollero et al., 2015).

The quantification of α -acetolactic acid and diacetyl was performed using the method described in a previously published paper (Ochando et al., 2018). The method is based on the derivatization of two samples with the 4,5-Dichloro-O-phenylenediamine (CAS 5348-42-5, $\geq 97.0\%$, Sigma-Aldrich®) followed by extraction with toluene in presence of diacetyl- d_6 as internal reference. The quantification was done with two samples: first for the content of free diacetyl (1) and the second after oxidation, for the total diacetyl (2) as the sum of the concentrations of free diacetyl and its precursor. The difference between (2) and (1) provided the quantity of α -acetolactate.

The determination of acetoin and 2,3-butanediol was also carried out by GC - MS (Ortega et al., 2001). The samples to be analyzed were pretreated by single liquid/liquid extraction with chloroform in presence of 1-hexanol as internal standard.

2.6. Statistical analysis

Each sample of separate fermentation triplicate was analyzed once. ANalysis Of VAriance (ANOVA) and Post Hoc Tests were carried out with the software Microsoft® Excel® 2013 version 15.0.5233.100.. Single factor ANOVA was performed to evaluated effect of SO₂ on each parameter measured. Difference among mean final concentrations of metabolites was determined using Tukey's test, significant results were considered at $p < 0.05$.

3. Results and discussion

3.1. Impact of the initial level of SO₂ on the alcoholic fermentation process

3.1.1. Combination of SO₂ with sugars

First, the combination kinetics of SO₂ with sugars were studied in simple medium containing water, sugars, malic and tartaric acid at pH 3.1. Depending on the process and the desired wine type, the initial clarification step of the must can last from a few hours to more than 24 hours under the influence of variable amounts of SO₂.

Therefore, the SO₂ combination kinetics in juice containing 180 g L⁻¹ total sugars were monitored over 24 hours with different initial levels of total sulfites: 20, 40, 60 or 80 mg L⁻¹. The juice was maintained at 20°C under an inert argon atmosphere. For each condition, the total SO₂ concentration remained almost unchanged, whereas the quantity of free SO₂ decreased rapidly during the first 5 hours, after which approximately 30% of the initial SO₂ was bound. After 24 hours, the reaction was almost stabilized, and 50% of the initial SO₂ was combined.

Glucose acts as an important binding agent of HSO₃⁻ when present at high concentrations in a must (Blouin, 2014). Indeed, 100 g L⁻¹ glucose can combine with

30 mg L⁻¹ SO₂, while fructose at 100 g L⁻¹ can only combine with 1.9 mg L⁻¹ SO₂. This difference is linked to the competition phenomenon between SO₂ binding compounds. If glucose is mixed with a compound (e.g., acetaldehyde) with more affinity for sulfur dioxide, it is the latter which combines first with the added sulfur dioxide (Gehman & Osman, 1954). The opposite is true with the fructose-SO₂ dissociation constant (K_d) of 15 mM lower than that of glucose-SO₂ (Blouin, 2014). On the assumption that SO₂ combines with glucose exclusively in the synthetic grape juice, we found a mean dissociation constant of 580 mM \pm 38 mM. This value is in agreement with the value of the equilibrium constant practically unchanged between pH 3 and 5.5 and equals about 0.61 (glucose = 1.1 M, added SO₂ = 0.005 M) (Vas, 1949). The slightly lower apparent K_d could be due to the more dilute solution used in our case (glucose = 0.5 M) and to the small binding contribution from fructose. Finally, we could also see that equilibrium was not yet fully achieved after 24 hours, especially when high concentrations of initial SO₂ were present, which can also explain why the K_d values were slightly different, although at the same order of magnitude (Vas, 1949).

3.1.2. Impact of SO₂ on the lag phase

To understand the impact of SO₂ on the lag phase, inoculation with yeast was performed 24 hours after initial SO₂ addition (0 to 40 mg L⁻¹) in the juice. The precise determination of the duration of the lag phase was performed using a tangent method. The lag phase duration corresponds to the value of the intersection between the growth phase tangent and the x-axis (time). At concentrations between 0 and 20 mg L⁻¹, SO₂ had little impact on the duration of the lag phase, whereas at concentrations above 25 mg L⁻¹, the lag phase duration was markedly increased

according to the level of SO₂, as shown in **Figure 1A**. If the duration of the lag phase was not considered, the fermentation kinetics were identical regardless of the different initial SO₂ doses (**Figure 1B**). The transition between the two responses to sulfites occurred at approximately 20 to 25 mg L⁻¹ initial SO₂ (**Figure 1C**). This threshold seems to reflect an important change in yeast metabolism. Regardless of the mode of SO₂ transport, sulfite is the dominant species of SO₂ inside the cell. As a highly reactive molecule, sulfite binds many metabolites and enzymes in the intracellular medium, explaining the observed lag phases. Sulfite can bind to proteins, coenzymes (NAD⁺ and FAD⁺), and co-factors such as vitamins, menadione and various metabolites (acetaldehyde, glucose, dihydroxyacetone-phosphate, pyruvate, oxaloacetic acid and α-ketoglutaric acid), thereby preventing their further use as substrates for metabolic pathways (Rankine & Pocock, 1969). The influx of SO₂ into eukaryotic cells also results in the immediate inhibition of glyceraldehyde-3-phosphate dehydrogenase (GAPDH) (Hinze & Holzer, 1986) (involved in the glycolysis pathway), ATPase, alcohol dehydrogenase and NAD⁺-glutamate dehydrogenase (Maier et al., 1986). Yeast tolerance to SO₂ is highly variable not only between species but also between strains. With the *S. cerevisiae* strain used in our case, the threshold sensibility seems to be near 20 to 25 mg L⁻¹ of total SO₂ added in the juice (**Figure 1C**).

3.1.3. Evolution of SO₂ during fermentation

The evolution of total SO₂ between the beginning and the stationary phase (80% of fermentation progress) was monitored (**Figure 2A**). Basically, the yeast produced approximately 16 mg L⁻¹ SO₂ in the absence of sulfite in the juice. This basic production of SO₂ by yeasts is intrinsically linked to the *de novo* formation of sulfur-

containing amino acids, in particular cysteine and methionine. Sulfur amino acids are scarce in the must; so they cannot entirely meet the sulfur requirements for protein synthesis of yeast. Therefore, yeasts find sulfur sources in the extracellular medium in the form of sulfates. Initially, sulfates are reduced into sulfites using two ATPs for the adenylation and phosphorylation of sulfate (SO_4^{2-}) step. Then, the product is reduced to bisulfite (HSO_3^-), which results in the oxidation of one NADPH. HSO_3^- can be converted into H_2S by sulfite reductases (encoded by the genes *MET10* and *MET5*) (Thomas & Surdin-Kerjan, 1997). Excess HSO_3^- and/or H_2S can be excreted in the medium. Thus, wine yeasts can be classified as low producers (few mg L^{-1}) or high producers of sulfites (more than 90 mg L^{-1}) from sulfate sources, depending on the fermentation conditions and the yeast strain (Eschenbruch & Bonish, 1976).

The final total SO_2 content increased with the total amount of SO_2 added at the start of the process (**Figure 2A**). However, the amount of SO_2 produced decreased by approximately 0.5 mg L^{-1} per gram of sulfites added (**Figure 2B**). At 30 mg L^{-1} , no variation in the level of SO_2 in the medium was found, and above this concentration, the total amount of SO_2 decreased during the fermentation process (indicating that SO_2 consumption is higher than its synthesis in these conditions). This constant decrease can be explained by the uptake of SO_2 from the synthetic grape juice into the cell during the lag phase (**Figure 3B, 3C, 3D**) in equilibrium with the reduction of sulfates into sulfites described previously. The mechanism of SO_2 and/or HSO_3^- cellular uptake is controversial: passive diffusion through the microbial cell membrane (Stratford & Rose, 1986), active transport (Pilkington & Rose, 1988) or carrier-mediated proton symport (Park & Bakalinsky, 2004). Once inside the cell, SO_2 dissociates into HSO_3^- and SO_3^{2-} because of the intracellular pH (5.5 - 6.5), and the

decrease in the intracellular molecular SO₂ concentration allows more molecular SO₂ to enter the cell.

3.1.4. SO₂ addition and acetaldehyde production

When SO₂ was added in the juice, fermentation only started when free SO₂ reached its minimal value, *i.e.*, below approximately 5 mg L⁻¹ (**Figure 3B, 3C, 3D**).

Concomitant with decreasing free SO₂, the production of acetaldehyde starts during the lag phase before any detectable CO₂ production (**Figure 3**). Then, acetaldehyde is mainly excreted during the growth period and its concentration is later decreased during the stationary phase. This observation agreed with abundant published data (Amerine & Ough, 1964; Fornachon, 1953; Ribéreau-Gayon et al., 1956a, 1956b; Weeks, 1969). While numerous works have shown that acetaldehyde accumulation mainly occurs during the growth period, there are very few published data concerning early acetaldehyde production at the onset of alcoholic fermentation (Cheraiti et al., 2010). Cheraiti *et al.* demonstrated that early acetaldehyde production is correlated with the lag phase duration, and this early acetaldehyde excretion is likely related to the detoxification of SO₂ (Cheraiti et al., 2010). In this way, acetaldehyde can be considered an early marker of the general fermenting activity of the yeast. The maximum accumulation of acetaldehyde was obtained a few hours after the maximum fermentation rate in all cases, and the maximum content of total acetaldehyde increased with the initial SO₂ content. The overproduction of total acetaldehyde was approximately 0.3 mg L⁻¹ per mg L⁻¹ SO₂ added. This is roughly consistent with the results of Jackowetz et al., who observed an increase of 0.366 mg acetaldehyde per mg SO₂ (Jackowetz et al., 2011). The overproduction of acetaldehyde in the presence of SO₂ could be due to (i) the inhibition of alcohol dehydrogenase, preventing acetaldehyde from being converted to ethanol, and/or (ii)

the binding of acetaldehyde to SO₂, resulting in a reduced amount to be metabolized into ethanol (Frivik & Ebeler, 2003). A correlation between initial SO₂ and total acetaldehyde at the end of the process was also observed, with acetaldehyde increasing by 1 mg L⁻¹ per 1.3 mg L⁻¹ SO₂ added. This last result is in accordance with the 1:1.4 (w/w) ratio calculated from the relative molecular weights of acetaldehyde and SO₂ (44:64) (Blouin, 2014). In *S. cerevisiae*, the formation of acetaldehyde during fermentation appears to be an effective means of controlling sulfite levels, as the two compounds react to form a stable and nontoxic product, 1-hydroxyethane sulfonate (Cheraiti et al., 2010). Therefore, the duration of the lag phase is related to the time required to eliminate the excessive intracellular concentration of HSO₃⁻. In addition, the increase in extracellular acetaldehyde causes binding to any free SO₂ and subsequent reduction of molecular SO₂ stress in the cell (Divol et al., 2012).

3.2. Production dynamics of free and total acetaldehyde

The production of free and total acetaldehyde was studied with 4 experimental modalities differentiated by the initial total SO₂ content in the juice ranging from 0 to 40 mg L⁻¹. Based on an original approach, the concentrations of free (with online gas monitoring) and total (with an enzymatic kit) acetaldehyde were followed jointly in the liquid phase during fermentation. The dynamics of the evolution of both compounds are presented in **Figure 4**. In all experiments, the global dynamics of production followed the same pattern: (1) a phase of accumulation in the medium during the first third of fermentation, corresponding to the growth phase of the yeast, and (2) a constant decrease during the stationary phase up to the end of the fermentation process. The evolution of the acetaldehyde concentrations (free and total) were relatively similar to the fermentation kinetics (**Figure 3**). A relationship exists between

the metabolic flux (dCO_2 / dt) and the concentration of acetaldehyde (Roustan & Sablayrolles, 2002). The production kinetic of acetaldehyde seems to be linked to the redox status of the cell. At the start of the process, the glycerol-pyruvate fermentation is a major contributor for recycling of NADH (Wang et al., 2001), which is consistent with the fact that glycerol accumulation stops at the end of the growth phase. In this case, acetaldehyde acts as a terminal electron acceptor for the redox balance of yeasts and their capacity to create energy by glycolysis (Liu & Pilone, 2000). In the second part of the fermentation process, acetaldehyde catabolism makes it possible the reoxidation of NADH into NAD^+ by ethanol synthesis catalyzed by ADH enzymes. The kinetics of the production of free and total acetaldehyde present a similar profile, with the maximum levels being reached at the end of the growth phase. However, for free acetaldehyde, there is no correlation between the maximum concentration and the initial SO_2 content. The maximum accumulation of free acetaldehyde in the medium (87 mg L^{-1}) was obtained with a 30 mg L^{-1} initial SO_2 content in the juice. For this sulfite level, the maximum free acetaldehyde content was approximately 50% higher than the levels reached in the modalities without and with $20 \text{ mg L}^{-1} SO_2$ and 25% higher than in the modality with 40 mg L^{-1} initial SO_2 .

Then, the proportion of bound acetaldehyde was calculated. The percentages of acetaldehyde in combination were very similar throughout fermentation in the modalities without and with 20 and $40 \text{ mg L}^{-1} SO_2$. Approximately 20% of the total acetaldehyde was combined at maximum accumulation, and this proportion increased to 50-60% at the end of fermentation. By contrast, for the modality with $30 \text{ mg L}^{-1} SO_2$, only 5% of the total acetaldehyde was bound at maximum accumulation. For this modality, during the stationary phase, the rate of combination remained lower compared to those under other fermentation conditions. Therefore, the modality with

an initial SO₂ dose of 30 mg L⁻¹ presented particularly novel and interesting characteristics, not only because there was no apparent variation of SO₂ during fermentation but also because acetaldehyde was mainly in free form during most of the process, as seen in **Figure 4**.

3.3. Impact of SO₂ on the production of α-acetolactic acid and derived higher alcohols

The production of α-acetolactic acid during fermentation conditions with various initial levels of SO₂ was also monitored (**Figure 5A**). The monitoring of this compound is of great interest because it is intrinsically related to acetaldehyde, and some aroma compounds are derived from it. Yeast produces this keto acid in two phases: the first occurs during the growth phase and the second one in the last stage of fermentation. At the end of the process, this compound is systematically reconsumed by the yeast. These production dynamics of α-acetolactate are consistent with previously reported data (Ochando et al., 2018). Some interesting differences can be observed with variation of the initial content of SO₂. In each case, the concentration at the end of the first phase of accumulation (growth phase) was very similar (0.5 to 0.6 mg L⁻¹). However, large differences appeared at the end of the second accumulation phase. The level of this keto acid in the modality with 30 mg L⁻¹ SO₂ was significantly much higher than that in the other fermentation conditions: 2 times higher than without or with 20 mg L⁻¹ SO₂ and 1.5 times higher than in the fermentation mixture initially containing 40 mg L⁻¹ sulfites. Therefore, there is a relationship between the dynamics of α-acetolactate and free acetaldehyde concentrations during fermentation. This is perfectly reasonable because the formation of α-acetolactic acid directly depends on

the formation of the acetaldehyde-TPP complex involving free acetaldehyde (Holzer et al., 1960, 1962; Holzer & Kohlhaw, 1961; Ullrich & Mannschreck, 1967).

The quantities of diacetyl produced differed with the initial level of SO₂ (**Figure 5B**). In modalities with high initial levels of SO₂ (30 and 40 mg L⁻¹), there was almost no diacetyl accumulation (below 40 µg L⁻¹) during fermentation, compared to the modalities without and with 20 mg L⁻¹ SO₂, in which the concentration of diacetyl increased to 180 µg L⁻¹. It is difficult to formulate a reliable hypothesis to explain these differences. However, it may be possible that a high level of SO₂ could protect α-acetolactic acid from oxidative decarboxylation into diacetyl.

At the end of fermentation, the concentrations of fermentative aromas originating from acetaldehyde and/or α-acetolactic acid were measured (**Table 1**). Compared to the sulfite-free modality, the production of isoamyl alcohol was increased by 17 to 25% in association with initial SO₂ contents of 40 and 30 mg L⁻¹, respectively. For isobutyl alcohol, these increases were equal to 42 and 34%, respectively. Moreover, this effect was detectable for the corresponding esters (*i.e.*, isoamyl and isobutyl acetates). For this four metabolites, statistical analysis enabled to form two distinct ($p < 0.05$ with Tuckey's tests) groups corresponding to low and high initial sulfite content in the must. The higher synthesis of isoamyl and isobutyl alcohols is not directly linked to SO₂ addition; it can be assumed that this overproduction is rather an indirect effect related to the modifications in the availability of free acetaldehyde and/or redox cofactors, as observed by (Bloem et al., 2016). Indeed, these authors have demonstrated that both the availability of precursors from central carbon metabolism and the accessibility of reduced cofactors contribute to volatile compound formation. The maximum production of 2,3-butanediol was significantly obtained at 30 mg L⁻¹ SO₂, with a 33% increase compared to the sulfite-free control. Butanediol derives

from the reduction of acetoin by the conversion of NADH to NAD⁺. Acetoin can be formed directly from the condensation of two acetaldehydes or from the decarboxylation of α -acetolactate (Romano & Suzzi, 1996). Thus, 2,3-butanediol production logically follows the same pattern as free acetaldehyde production. The modality with 30 mg L⁻¹ initial SO₂ was clearly distinct in that (1) the level of sulfites remained stable throughout fermentation, and (2) the production of metabolic intermediates (free acetaldehyde and α -acetolactate) was higher than in the other conditions tested. Modification of the regulation of metabolic pathways around the acetaldehyde node results in differences in the synthesis of isoamyl and isobutyl alcohols. These last variations certainly cannot be attributed to differences in the regulation of nitrogen metabolism because, under the conditions examined in this study, no variability was observed in the fermentation kinetics or cell population (data not shown) or, thus, valine, leucine or isoleucine consumption.

3.4. Effect of SO₂ on the redox balance of NADPH/NADP⁺

SO₂ addition also had an impact on the synthesis of other metabolites that are not directly linked to acetaldehyde: methionol, phenyl ethanol and phenyl ethyl acetate. The final concentration of these volatile molecules increased with the initial SO₂ content (**Table 1**). For example, the concentration of methionol was increased by 55% in the presence of 40 mg L⁻¹ initial SO₂ compared to sulfite-free fermentation. Methionol is produced from an amino acid containing sulphur, L-methionine, through the Ehrlich pathway. The L-methionine requirement for yeast growth is greater than the available resources (Crépin et al., 2017), and L-methionine was depleted in all our modalities. Therefore, the final methionol concentrations were linked to differences in its biosynthesis. Global glycolysis and especially glyceraldehyde-3-phosphate

dehydrogenase is inhibited at high concentrations of free SO₂ (Maier et al., 1986). Under these inhibiting conditions, the production of acetaldehyde by yeast for combination with SO₂ is limited. In the conditions with 40 mg L⁻¹ initial SO₂, the total acetaldehyde content in the medium was very low during the lag phase, as shown in **Figure 4A**. To decrease the level of free SO₂, yeast should use another strategy for detoxification of the medium: consumption of SO₂ to form L-methionine. This higher flux of L-methionine at high SO₂ level induces a higher final concentration of methionol.

It is important to note that *de novo* L-methionine biosynthesis *via* the assimilation of inorganic sulfate requires three molecules of NADPH per molecule of L-methionine (Stincone et al., 2015) (**Figure 6**). Therefore, in the case of high sulfite levels, it can be hypothesized a greater demand in NADPH. To regenerate NADPH, yeast usually use the pentose phosphate pathway (PPP) (**Figure 6**). A higher flux through the PPP results in higher accumulation of phenyl ethanol and its corresponding ester (phenyl ethyl acetate) (Cadière et al., 2011). In our work, the high levels of these two volatile compounds at high SO₂ content (40 mg L⁻¹) support this hypothesis. Therefore, greater *de novo* synthesis of phenylpyruvate by the PPP can explain the evolution of phenyl ethanol production with the increase in free SO₂. This higher production of phenylpyruvate at high concentrations of SO₂ is also observed in the literature (Herraiz et al., 1989). Moreover, other studies (Vigentini et al., 2013) have shown in higher ribitol (derivative of PPP and ribulose) accumulation in *Brettanomyces bruxellensis* when the yeast was exposed to sulfites.

Comparison of the evolution of the pool of certain aroma compounds under different initial concentrations of SO₂ enables to set up hypotheses allowing a better understanding of yeast metabolism. Without SO₂ or in the presence of a low SO₂

content, yeast cells need to import sulfates for sulfur metabolism. This results in the production of sulfites, which are “neutralized” by the production of acetaldehyde. In contrast, at high SO₂ levels, yeast must reduce cellular stress and “consume” sulfites, leading to (1) an increase in methionol synthesis and (2) a higher flux of the pentose phosphate pathway to regenerate more NADPH, resulting in increased accumulation of both phenyl ethanol and phenyl ethyl acetate.

Yeast consumes SO₂ to detoxify the medium, resulting in a significant change in the regulation of sulfur metabolism and major disruptions in the NADPH/NADP⁺ redox equilibrium, altering the production of several aroma compounds.

3.5. Addition of acetaldehyde and sodium 1-hydroxyethanesulphonate

Through previous experiments, the importance of SO₂ and acetaldehyde in the physiological state of yeast and the resulting sensory profiles of wines has been highlighted. At this stage, it is particularly interesting to expand our understanding of the roles of free and bound acetaldehyde because these two forms certainly do not have the same consequences for yeast metabolism. For this purpose, the addition of free and bound acetaldehyde (in the form of sodium 1-hydroxyethanesulphonate, 1-HES) was performed at the beginning of the second phase of the accumulation of α -acetolactic acid, *i.e.*, when its impact would be the most visible. The objective was to visualize the effect of the form of acetaldehyde on the production of this keto acid. The range of added acetaldehyde concentrations was chosen to avoid detrimental effects on fermentation kinetics (Roustan & Sablayrolles, 2002). The total acetaldehyde concentration and diacetyl production were also monitored (**Figure 7**).

Regardless of the initial concentration of free acetaldehyde, complete consumption by yeast was observed in less than 24 hours (**Figure 7, A1**). In contrast, after the addition of 1-HES, the concentration of total acetaldehyde remained stable until the end of fermentation (**Figure 7, B1**). When 1-HES was added, the final concentration of total SO₂ corresponded to the sum of the SO₂ added with 1-HES (linked to the synthesis of the product) and the 15 mg L⁻¹ SO₂ produced by the strain from the sulfate pool (**Table 2**). This last finding confirmed that 1-HES remained intact during fermentation. Thus, these data show that yeast cannot use acetaldehyde when it is bound to SO₂.

After the addition of free acetaldehyde, we observed a transient increase in α -acetolactate and diacetyl concentrations (**Figure 7, A2 and A3**). Contrary to the observations made under different initial concentrations of SO₂, the addition of free acetaldehyde to the medium resulted in higher production of diacetyl. This difference may be explained by the fact that, following free acetaldehyde addition, the SO₂ concentration remained low and did not protect α -acetolactate against oxidative decarboxylation. In contrast, after the addition of 1-HES, no increase in α -acetolactate or diacetyl in the medium was observed (**Figure 7, B2 and B3**). As 1-HES is not utilized by the yeast, it is logical that the amounts of both compounds remained similar to those in the control.

4. Conclusion

This work shows the impact of the initial content of SO₂ on fermentation kinetics and yeast metabolism. Our results suggest that the initial content of SO₂ not only affects the synthesis of sulfur metabolites but also impacts the overall sensory profile of wines. Our data also show the necessity of differentiating the different forms of

acetaldehyde and SO₂ to achieve progress in understanding fermentation kinetics and yeast metabolism. Future work will be dedicated to other yeast strains to study the genericity of the observed behaviors. For this purpose, online monitoring of the production dynamics of free acetaldehyde by monitoring the gas generated compared to the bound acetaldehyde content constitutes a new approach that is particularly interesting for better understanding the dynamics of SO₂ and free acetaldehyde production.

Acknowledgements

We thank Yannick Sire for the analyses of SO₂ and acetaldehyde.

We thank Christine Le Guernevé for performing NMR analyses.

References

- Aguera, E., Sire, Y., Mouret, J.-R., Sablayrolles, J.-M., & Farines, V. (2018). Comprehensive Study of the Evolution of the Gas–Liquid Partitioning of Acetaldehyde during Wine Alcoholic Fermentation. *Journal of Agricultural and Food Chemistry*, 66(24), 6170-6178. <https://doi.org/10.1021/acs.jafc.8b01855>
- Amerine, M. A., & Ough, C. S. (1964). Studies with Controlled Fermentation. VIII. Factors Affecting Aldehyde Accumulation. *American Journal of Enology and Viticulture*, 15(1), 23-33.
- Aranda, A., Jiménez-Martí, E., Orozco, H., Matallana, E., & del Olmo, M. (2006). Sulfur and Adenine Metabolisms Are Linked, and Both Modulate Sulfite Resistance in Wine Yeast. *Journal of Agricultural and Food Chemistry*, 54(16), 5839-5846. <https://doi.org/10.1021/jf060851b>
- Bakker, J., & Timberlake, C. F. (1997). Isolation, Identification, and Characterization of New Color-Stable Anthocyanins Occurring in Some Red Wines. *Journal of Agricultural and Food Chemistry*, 45(1), 35-43. <https://doi.org/10.1021/jf960252c>

- Bely, M., Sablayrolles, J. M., & Barre, P. (1990). Description of Alcoholic Fermentation Kinetics : Its Variability and Significance. *American Journal of Enology and Viticulture*, 41(4), 319-324.
- Bloem, A., Sanchez, I., Dequin, S., & Camarasa, C. (2016). Metabolic Impact of Redox Cofactor Perturbations on the Formation of Aroma Compounds in *Saccharomyces cerevisiae*. *Applied and Environmental Microbiology*, 82(1), 174-183.
<https://doi.org/10.1128/AEM.02429-15>
- Blouin, J. (2014). *Le SO₂ en oenologie*. Dunod.
- Burroughs, L. F., & Sparks, A. H. (1973). Sulphite-binding power of wines and ciders. II. Theoretical consideration and calculation of sulphite-binding equilibria. *Journal of the Science of Food and Agriculture*, 24(2), 199-206.
<https://doi.org/10.1002/jsfa.2740240212>
- Cadière, A., Ortiz-Julien, A., Camarasa, C., & Dequin, S. (2011). Evolutionary engineered *Saccharomyces cerevisiae* wine yeast strains with increased in vivo flux through the pentose phosphate pathway. *Metabolic Engineering*, 13(3), 263-271.
<https://doi.org/10.1016/j.ymben.2011.01.008>
- Cheraiti, N., Guezennec, S., & Salmon, J.-M. (2010). Very early acetaldehyde production by industrial *Saccharomyces cerevisiae* strains : A new intrinsic character. *Applied Microbiology and Biotechnology*, 86(2), 693-700. <https://doi.org/10.1007/s00253-009-2337-5>
- Cheyrier, V., Dueñas-Paton, M., Salas, E., Maury, C., Souquet, J. M., Sarni-Manchado, P., & Fulcrand, H. (2006). Structure and properties of wine pigments and tannins. *American Journal of Enology and Viticulture*, 57(3), 298-305.
- Crépin, L., Truong, N. M., Bloem, A., Sanchez, I., Dequin, S., & Camarasa, C. (2017). Management of Multiple Nitrogen Sources during Wine Fermentation by *Saccharomyces cerevisiae*. *Applied and Environmental Microbiology*, 83(5), e02617-16. <https://doi.org/10.1128/AEM.02617-16>

- Divol, B., du Toit, M., & Duckitt, E. (2012). Surviving in the presence of sulphur dioxide : Strategies developed by wine yeasts. *Applied Microbiology and Biotechnology*, 95(3), 601-613. <https://doi.org/10.1007/s00253-012-4186-x>
- Donalies, U. E. B., & Stahl, U. (2002). Increasing sulphite formation in *Saccharomyces cerevisiae* by overexpression of MET14 and SSU1. *Yeast*, 19(6), 475-484. <https://doi.org/10.1002/yea.849>
- Eschenbruch, R., & Bonish, P. (1976). Production of sulphite and sulphide by low-and high-sulphite forming wine yeasts. *Archives of Microbiology*, 107(3), 299-302. <https://doi.org/10.1007/BF00425343>
- Ferreira, D., Galeote, V., Sanchez, I., Legras, J.-L., Ortiz-Julien, A., & Dequin, S. (2017). Yeast multistress resistance and lag-phase characterisation during wine fermentation. *FEMS Yeast Research*, 17(6). <https://doi.org/10.1093/femsyr/fox051>
- Ferreira-Lima, N., Vallverdú-Queralt, A., Meudec, E., Mazauric, J.-P., Sommerer, N., Bordignon-Luiz, M. T., Cheynier, V., & Le Guernevé, C. (2016). Synthesis, Identification, and Structure Elucidation of Adducts Formed by Reactions of Hydroxycinnamic Acids with Glutathione or Cysteinylglycine. *Journal of Natural Products*, 79(9), 2211-2222. <https://doi.org/10.1021/acs.jnatprod.6b00279>
- Fornachon, J. (1953). The Accumulation of Acetaldehyde by Suspensions of Yeasts. *Australian Journal of Biological Sciences*, 6(2), 222. <https://doi.org/10.1071/BI9530222>
- Frivik, S., & Ebeler, S. (2003). Influence of sulfur dioxide on the formation of aldehydes in white wine. *American Journal of Enology and Viticulture*, 54, 31-38.
- Gehman, H., & Osman, E. M. (1954). The Chemistry of the Sugar-Sulfite Reaction and Its Relationship to Food Problems. In *Advances in Food Research* (Vol. 5, p. 53-96). Elsevier. [https://doi.org/10.1016/S0065-2628\(08\)60221-9](https://doi.org/10.1016/S0065-2628(08)60221-9)
- Herraiz, T., Martin-Alvarez, P. J., Reglero, G., Herraiz, M., & Cabezudo, M. D. (1989). Differences between wines fermented with and without sulphur dioxide using various

- selected yeasts. *Journal of the Science of Food and Agriculture*, 49(2), 249-258.
<https://doi.org/10.1002/jsfa.2740490213>
- Hinze, H., & Holzer, H. (1986). Analysis of the energy metabolism after incubation of *Saccharomyces cerevisiae* with sulfite or nitrite. *Archives of Microbiology*, 145(1), 27-31. <https://doi.org/10.1007/BF00413023>
- Holzer, H., Fonseca-Wollheim, F., Kohlhaw, G., & Woenckhaus, Ch. W. (1962). Active forms of acetaldehyde, pyruvate and glycolic acetaldehyde. *Annals of the New York Academy of Sciences*, 98(2), 453-465. <https://doi.org/10.1111/j.1749-6632.1962.tb30566.x>
- Holzer, H., Goedde, H. W., Göggel, K.-H., & Ulrich, B. (1960). Identification of α -hydroxyethyl thiamine pyrophosphate ("active acetaldehyde") as an intermediate in the oxidation of pyruvate by pyruvic oxidase from yeast mitochondria. *Biochemical and Biophysical Research Communications*, 3(6), 599-602. [https://doi.org/10.1016/0006-291X\(60\)90069-3](https://doi.org/10.1016/0006-291X(60)90069-3)
- Holzer, H., & Kohlhaw, G. (1961). Enzymatic formation of α -acetolactate from α -hydroxyethyl-2-thiamine pyrophosphate ("active acetaldehyde") and pyruvate. *Biochemical and Biophysical Research Communications*, 5(6), 452-456.
[https://doi.org/10.1016/0006-291X\(61\)90094-8](https://doi.org/10.1016/0006-291X(61)90094-8)
- Jackowetz, J. N., Dierschke, S., & Mira de Orduña, R. (2011). Multifactorial analysis of acetaldehyde kinetics during alcoholic fermentation by *Saccharomyces cerevisiae*. *Food Research International*, 44(1), 310-316.
<https://doi.org/10.1016/j.foodres.2010.10.014>
- Liu, S.-Q., & Pilone, G. J. (2000). An overview of formation and roles of acetaldehyde in winemaking with emphasis on microbiological implications. *International journal of food science & technology*, 35(1), 49–61. <https://doi.org/10.1046/j.1365-2621.2000.00341.x>

- Maier, K., Hinze, H., & Leuschel, L. (1986). Mechanism of sulfite action on the energy metabolism of *Saccharomyces cerevisiae*. *Biochimica et Biophysica Acta (BBA) - Bioenergetics*, 848(1), 120-130. [https://doi.org/10.1016/0005-2728\(86\)90167-2](https://doi.org/10.1016/0005-2728(86)90167-2)
- Morakul, S., Mouret, J.-R., Nicolle, P., Trelea, I. C., Sablayrolles, J.-M., & Athes, V. (2011). Modelling of the gas–liquid partitioning of aroma compounds during wine alcoholic fermentation and prediction of aroma losses. *Process Biochemistry*, 46(5), 1125-1131. <https://doi.org/10.1016/j.procbio.2011.01.034>
- Ochando, T., Mouret, J.-R., Humbert-Goffard, A., Sablayrolles, J.-M., & Farines, V. (2016). Impact of initial lipid content and oxygen supply on alcoholic fermentation in champagne-like musts. *Food Research International*. <https://doi.org/10.1016/j.foodres.2016.11.010>
- Ochando, T., Mouret, J.-R., Humbert-Goffard, A., Sablayrolles, J.-M., & Farines, V. (2018). Vicinal diketones and their precursors in wine alcoholic fermentation : Quantification and dynamics of production. *Food Research International*, 103, 192-199. <https://doi.org/10.1016/j.foodres.2017.10.040>
- Ortega, C., López, R., Cacho, J., & Ferreira, V. (2001). Fast analysis of important wine volatile compounds. *Journal of Chromatography A*, 923(1-2), 205-214. [https://doi.org/10.1016/S0021-9673\(01\)00972-4](https://doi.org/10.1016/S0021-9673(01)00972-4)
- Park, H., & Bakalinsky, A. (2004). Evidence for sulfite proton symport in *Saccharomyces cerevisiae*. *Journal of Microbiology and Biotechnology*, 14, 967-971.
- Pilkington, B. J., & Rose, A. H. (1988). Reactions of *Saccharomyces cerevisiae* and *Zygosaccharomyces bailii* to Sulphite. *Microbiology*, 134(10), 2823-2830. <https://doi.org/10.1099/00221287-134-10-2823>
- Pronk, J. T., Yde Steensma, H., & Van Dijken, J. P. (1996). Pyruvate metabolism in *Saccharomyces cerevisiae*. *Yeast (Chichester, England)*, 12(16), 1607-1633. [https://doi.org/10.1002/\(sici\)1097-0061\(199612\)12:16<1607::aid-yea70>3.0.co;2-4](https://doi.org/10.1002/(sici)1097-0061(199612)12:16<1607::aid-yea70>3.0.co;2-4)

- Rankine, B. C., & Pocock, K. F. (1969). Influence of yeast strain on binding of sulphur dioxide in wines, and on its formation during fermentation. *Journal of the Science of Food and Agriculture*, 20(2), 104-109. <https://doi.org/10.1002/jsfa.2740200210>
- Rehm, H.-J., & Wittmann, H. (1962). Beitrag zur Kenntnis der antimikrobiellen Wirkung der schwefligen Säure I. Mitteilung Übersicht über einflussnehmende Faktoren auf die antimikrobielle Wirkung der schwefligen Säure. *Zeitschrift für Lebensmittel-Untersuchung und -Forschung*, 118(5), 413-429. <https://doi.org/10.1007/BF01104424>
- Ribéreau-Gayon, J., Peynaud, E., & Lafon, M. (1956a). Investigations on the origin of secondary products of alcoholic fermentation. *American Journal of Enology and Viticulture*, 7, 53-61.
- Ribéreau-Gayon, J., Peynaud, E., & Lafon, M. (1956b). Investigations on the Origin of Secondary Products of Alcoholic Fermentation. Part II. *American Journal of Enology and Viticulture*, 7(3), 112-118.
- Rollero, S., Bloem, A., Camarasa, C., Sanchez, I., Ortiz-Julien, A., Sablayrolles, J.-M., Dequin, S., & Mouret, J.-R. (2015). Combined effects of nutrients and temperature on the production of fermentative aromas by *Saccharomyces cerevisiae* during wine fermentation. *Applied Microbiology and Biotechnology*, 99(5), 2291-2304. <https://doi.org/10.1007/s00253-014-6210-9>
- Romano, P., & Suzzi, G. (1996). Origin and production of acetoin during wine yeast fermentation. *Applied and Environmental Microbiology*, 62(2), 309.
- Roustan, J. L., & Sablayrolles, J.-M. (2002). Modification of the acetaldehyde concentration during alcoholic fermentation and effects on fermentation kinetics. *Journal of Bioscience and Bioengineering*, 93(4), 367-375. [https://doi.org/10.1016/S1389-1723\(02\)80069-X](https://doi.org/10.1016/S1389-1723(02)80069-X)
- Stincone, A., Prigione, A., Cramer, T., Wamelink, M. M. C., Campbell, K., Cheung, E., Olin-Sandoval, V., Grüning, N.-M., Krüger, A., Tauqeer Alam, M., Keller, M. A., Breitenbach, M., Brindle, K. M., Rabinowitz, J. D., & Ralser, M. (2015). The return of metabolism : Biochemistry and physiology of the pentose phosphate pathway: The

- pentose phosphate pathway. *Biological Reviews*, 90(3), 927-963.
<https://doi.org/10.1111/brv.12140>
- Stratford, M., & Rose, A. H. (1986). Transport of Sulphur Dioxide by *Saccharomyces cerevisiae*. *Microbiology*, 132(1), 1-6. <https://doi.org/10.1099/00221287-132-1-1>
- Swiegers, J. H., Bartowsky, E. J., Henschke, P. A., & Pretorius, I. S. (2005). Yeast and bacterial modulation of wine aroma and flavour. *Australian Journal of grape and wine research*, 11(2), 139–173. <https://doi.org/10.1111/j.1755-0238.2005.tb00285.x>
- Thomas, D., & Surdin-Kerjan, Y. (1997). Metabolism of sulfur amino acids in *Saccharomyces cerevisiae*. *Microbiology and Molecular Biology Reviews*, 61(4), 503-532. PMC.
- Ullrich, J., & Mannschreck, A. (1967). Studies on the Properties of (-)-2- α -Hydroxyethyl-Thiamine Pyrophosphate (« Active Acetaldehyde »). *European Journal of Biochemistry*, 1(1), 110-116. <https://doi.org/10.1111/j.1432-1033.1967.tb00051.x>
- Vas, K. (1949). The equilibrium between glucose and sulphurous acid. *Journal of the Society of Chemical Industry*, 68(12), 340-343. <https://doi.org/10.1002/jctb.5000681203>
- Vigentini, I., Lucy Joseph, C. M., Picozzi, C., Foschino, R., & Bisson, L. F. (2013). Assessment of the *Brettanomyces bruxellensis* metabolome during sulphur dioxide exposure. *FEMS Yeast Research*, 13(7), 597-608. <https://doi.org/10.1111/1567-1364.12060>
- Wang, Z., Zhuge, J., Fang, H., & Prior, B. A. (2001). Glycerol production by microbial fermentation. *Biotechnology Advances*, 19(3), 201-223.
[https://doi.org/10.1016/S0734-9750\(01\)00060-X](https://doi.org/10.1016/S0734-9750(01)00060-X)
- Weeks, C. (1969). Production of sulfur dioxide-binding compounds and of sulfur dioxide by two *Saccharomyces* yeasts. *American Journal of Enology and Viticulture*, 20, 32-39.
- Zoecklein, B. W., Fugelsang, K. C., Gump, B. H., & Nury, F. S. (1999). *Wine Analysis and Production*. Springer US. <https://doi.org/10.1007/978-1-4757-6967-8>

Figure captions

Figure 1: Comparison of the release of CO₂ according to the time of fermentation (including the lag phase duration) **(A)** and the normalized time of fermentation (without the lag phase duration) **(B)**, for the control without SO₂ (◊) and for conditions involving 10 (◊), 15 (◊), 20 (◊), 25 (◊), 30 (◊), 35 (◊), or 40 (◊) mg L⁻¹ initial SO₂. **(C)** The linear regression of the duration of the lag phase as a function of the level of total SO₂ at the beginning of fermentation with between 0 and 20 mg L⁻¹ SO₂ shows a value of $r^2=0.9331$, and that above 25 mg L⁻¹ SO₂ is $r^2 = 0.9908$.

Figure 2: **(A)** Dynamics of the evolution of total SO₂ during alcoholic fermentation for 0 (◊), 20 (◊), 30 (◊), and 40 (◊) mg L⁻¹ initial SO₂. **(B)** Δ Total SO₂ = Final Total SO₂ (measured during the stationary phase) – Initial Total SO₂ (added in the juice). The correlation coefficient is $r^2 = 0.989$.

Figure 3: Evolution of free SO₂ (◊, left axis), fermentation rate (●, right axis) and total acetaldehyde (◊, right axis) during alcoholic fermentation in the presence of 0 **(A)**, 20 **(B)**, 30 **(C)** and 40 **(D)** mg L⁻¹ initial SO₂.

The standard deviation is 4.8% for total SO₂ and 2.8% for total acetaldehyde (n=3).

Figure 4: Evolution dynamics of free (full line) and total (diamond and dotted line) acetaldehyde in the presence of 0 (◊), 20 (◊), 30 (◊), and 40 (◊) mg L⁻¹ initial SO₂ over time.

The standard deviations are 2.8% and 9% for total and free acetaldehyde, respectively (n=3).

Figure 5: Evolution dynamics of α -acetolactic acid (**A**) and diacetyl (**B**) in the presence of 0 (\diamond), 20 (\blacklozenge), 30 (\blacklozenge), and 40 (\blacklozenge) mg L^{-1} initial SO_2 .

The standard deviation is 5% for $n=3$.

Figure 6: Pentose phosphate pathway (PPP) from glucose to chorismate, with the partial glycolysis pathway represented in the gray frame. Dashed lines correspond to successive enzymatic reactions.

Figure 7: Evolution dynamics of total acetaldehyde (**A1** and **B1**), α -acetolactatic acid (**A2** and **B2**) and diacetyl (**A3** and **b3**) after the addition of 0 (\blacklozenge), 2 (\blacklozenge), 4.5 (\blacklozenge and \blacklozenge) or 6.8 (\blacklozenge) mM free acetaldehyde and 0 (\blacklozenge), 2 (\blacklozenge), 4.6 (\blacklozenge) or 7 (\blacklozenge) mM sodium 1-hydroxyethanesulphonate (1-HES).

The standard deviation is 2.8% for total acetaldehyde and 5% for α -acetolactic acid and diacetyl ($n=3$).

Table 1: Final concentrations of fermentation metabolites (mg L^{-1}) with associate standard deviations from triplicate of experiments. Different letters indicate significant difference ($p < 0.05$) among quantitative variables.

SO_2 (mg L^{-1})	0	20	30	40
Free acetaldehyde	8.3 ± 0.6 a	8.3 ± 0.3 a	8.1 ± 0.6 a	24.2 ± 1.9 b
Total acetaldehyde	19.2 ± 1.4 a	29.8 ± 1.8 b	41.9 ± 2.3 c	50.1 ± 3.9 d
α -Acetolactate	0.01 ± 0.001 a	0.01 ± 0.001 a	0.07 ± 0.003 b	0.05 ± 0.004 ab
Diacetyl	0.04 ± 0.001 a	0.032 ± 0.002 a	0 b	0 b
Isoamyl alcohol	76.3 ± 3.7 a	81.8 ± 6.4 a	95.8 ± 7.0 b	89.8 ± 6.2 b
Isobutyl alcohol	10.4 ± 0.6 a	11.0 ± 0.9 a	14.8 ± 0.7 b	13.9 ± 0.4 b
Isoamyl acetate	2.54 ± 0.10 a	2.57 ± 0.20 a	5.45 ± 0.43 b	5.06 ± 0.37 b
Isobutyl acetate	0.04 ± 0.002 a	0.05 ± 0.003 a	0.15 ± 0.006 b	0.16 ± 0.012 b
2,3-Butanediol	235.1 ± 13.6 a	200.2 ± 15.4 a	313.6 ± 10.0 b	194.6 ± 12.6 a
Methionol	1.03 ± 0.08 a	1.07 ± 0.08 a	1.41 ± 0.10 ab	1.59 ± 0.12 b
Phenyl ethanol	8.4 ± 0.3 a	7.7 ± 0.3 a	9.7 ± 0.8 ab	10.2 ± 0.5 b
Phenyl ethyl acetate	0.34 ± 0.02 a	0.31 ± 0.02 a	0.60 ± 0.04 b	0.66 ± 0.05 b

Table 2: Final concentrations of total SO₂ in mg L⁻¹ with associate standard deviations from triplicate of experiments. For the addition of sodium 1-hydroxyethanesulphonate (1-HES), the theoretical value corresponds to the amount of SO₂ added (in bound form), and the measured value corresponds to SO₂ detected in the potentiometric assay, less the value in the control.

Modality	Without addition	Addition of free acetaldehyde	Addition of 1-HES	
	Total SO ₂ mg L ⁻¹		SO ₂ Theoretical mg L ⁻¹	SO ₂ Measured mg L ⁻¹
Control	13.1 ± 0.3			
Addition* 1		12.4 ± 0.7	144 ± 4.8	141 ± 3.7
Addition* 2		13.4 ± 0.7	290 ± 20.6	281 ± 18.5
Addition* 3		12.4 ± 0.9	427 ± 21.8	432 ± 28.5

**: of free acetaldehyde or 1-HES*

Figure 1.

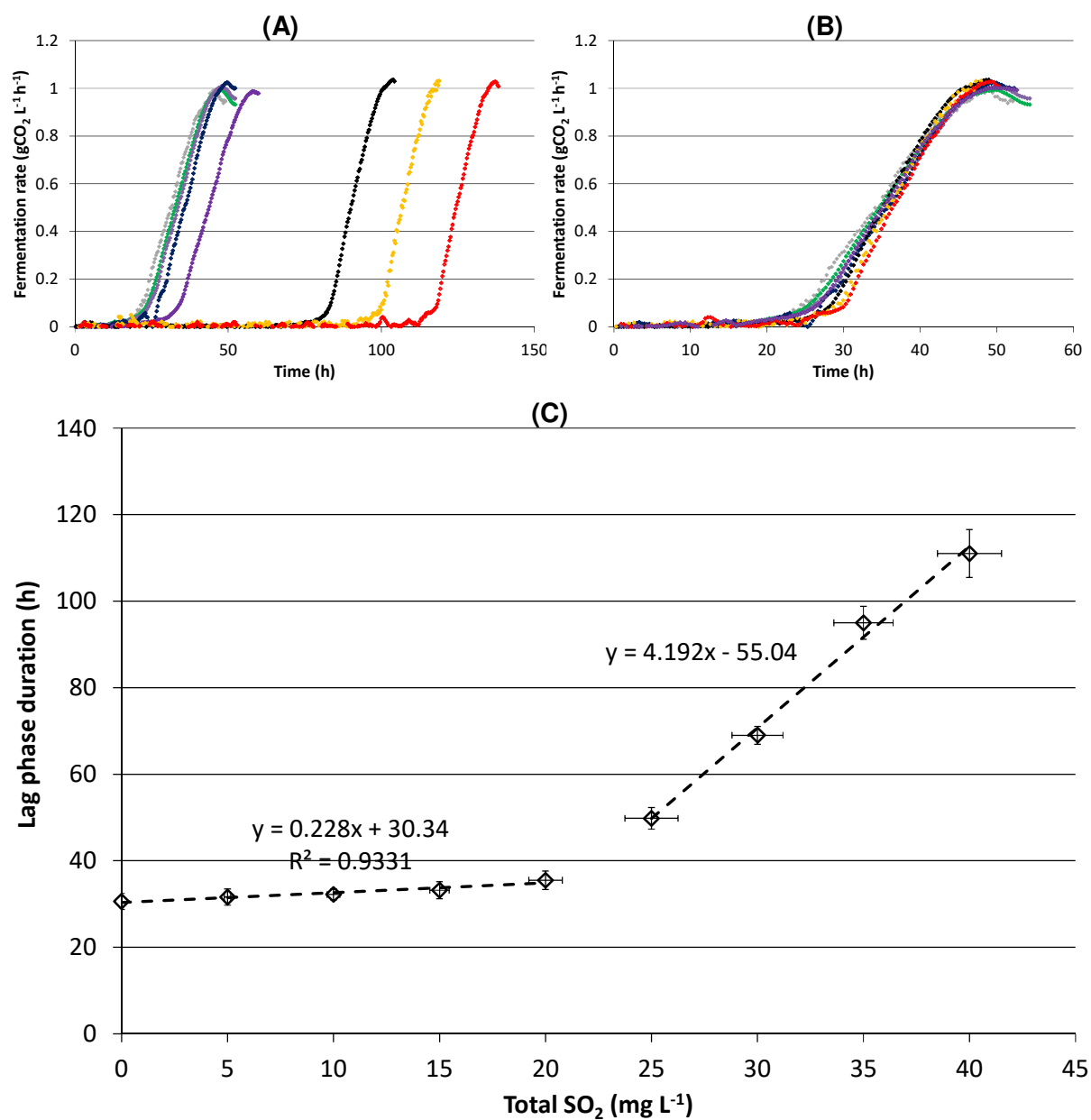


Figure 2.

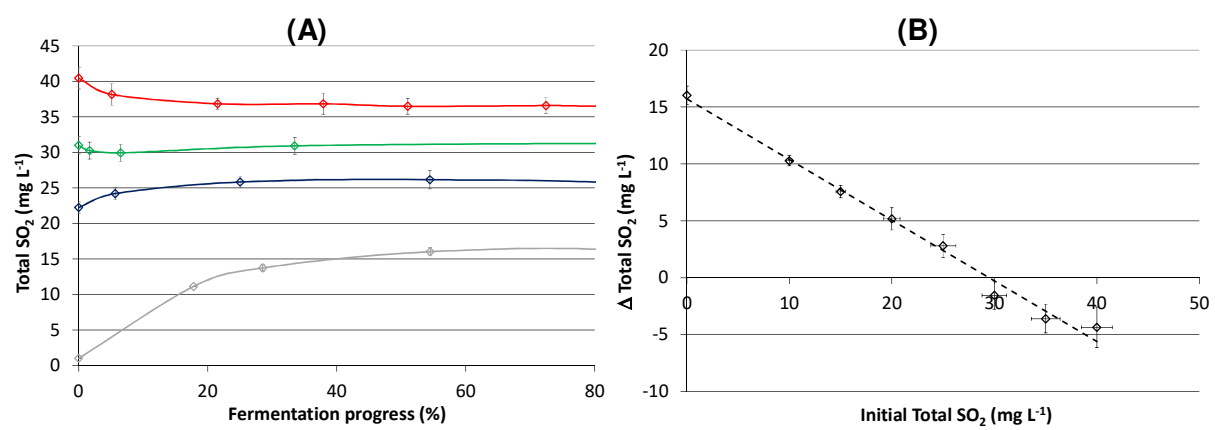


Figure 3.

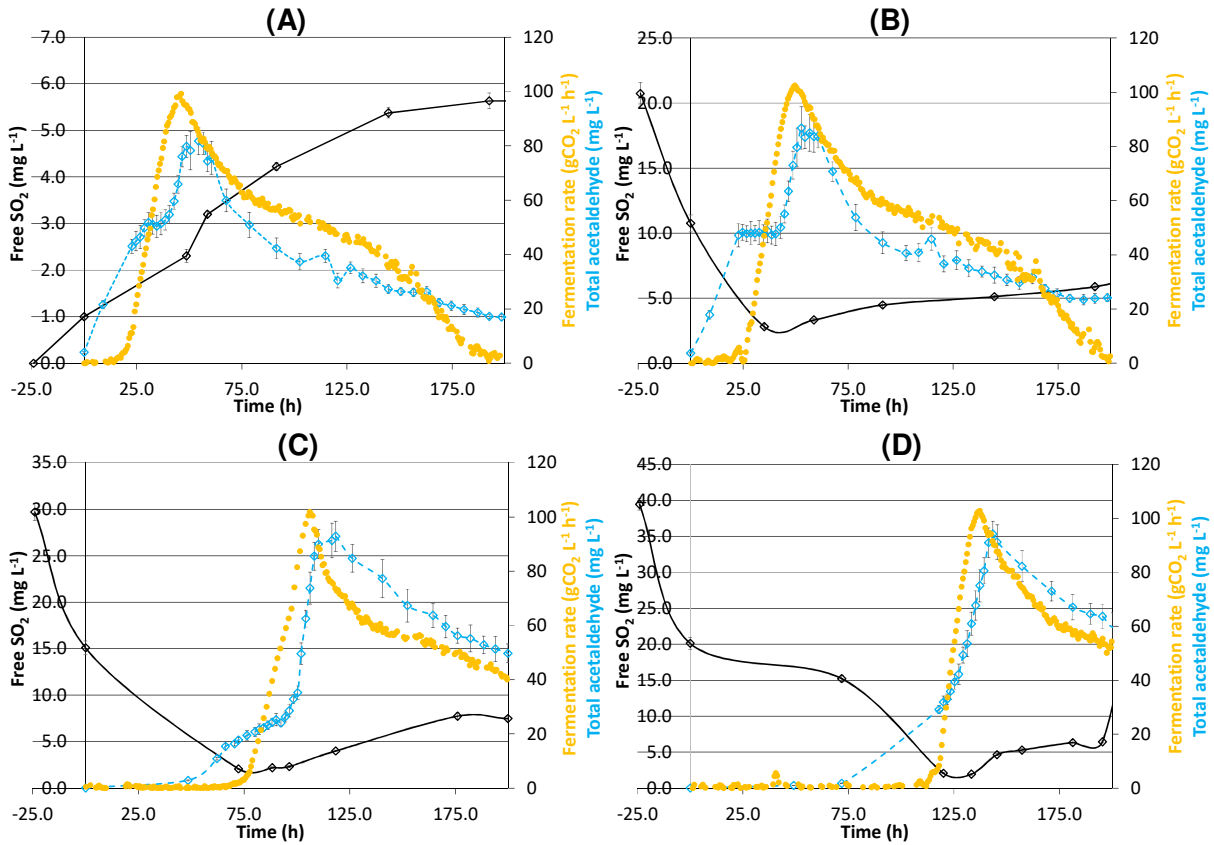


Figure 4.

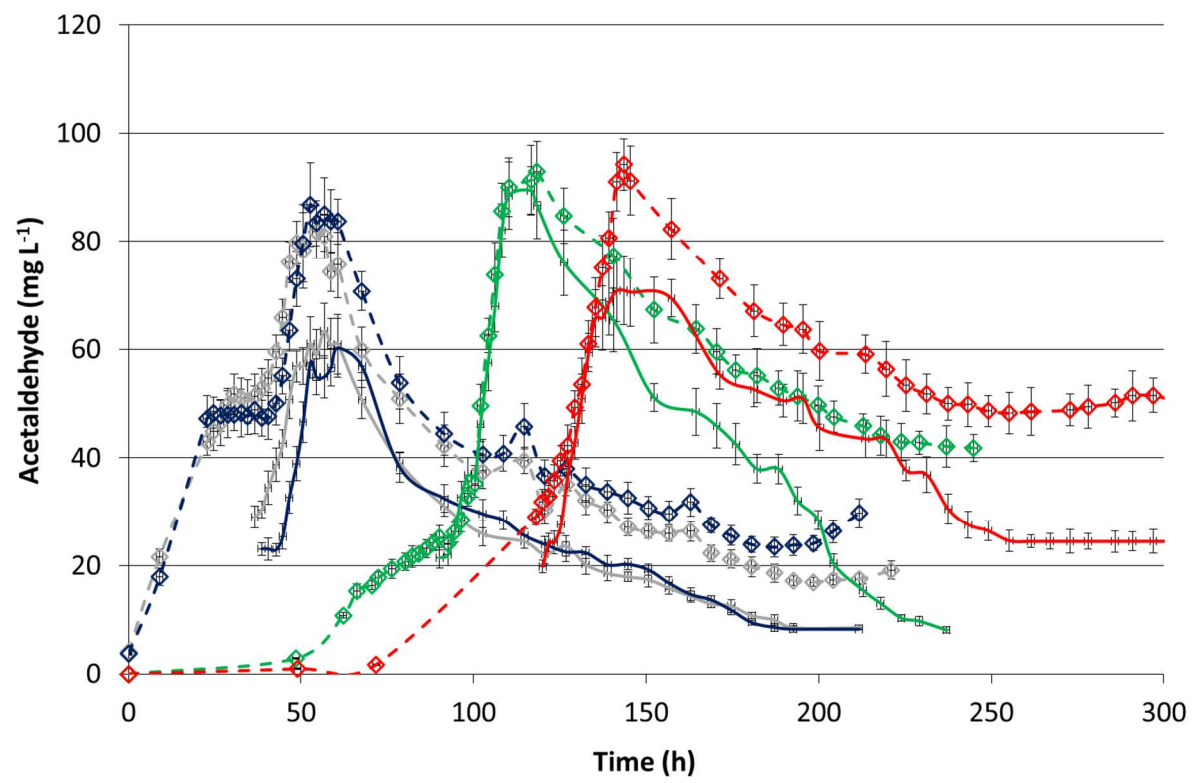


Figure 5.

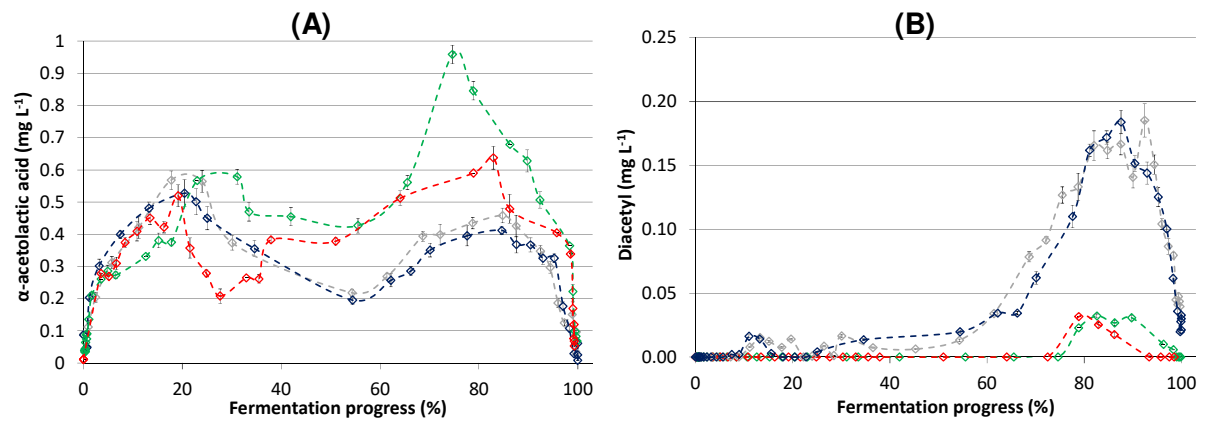


Figure 6.

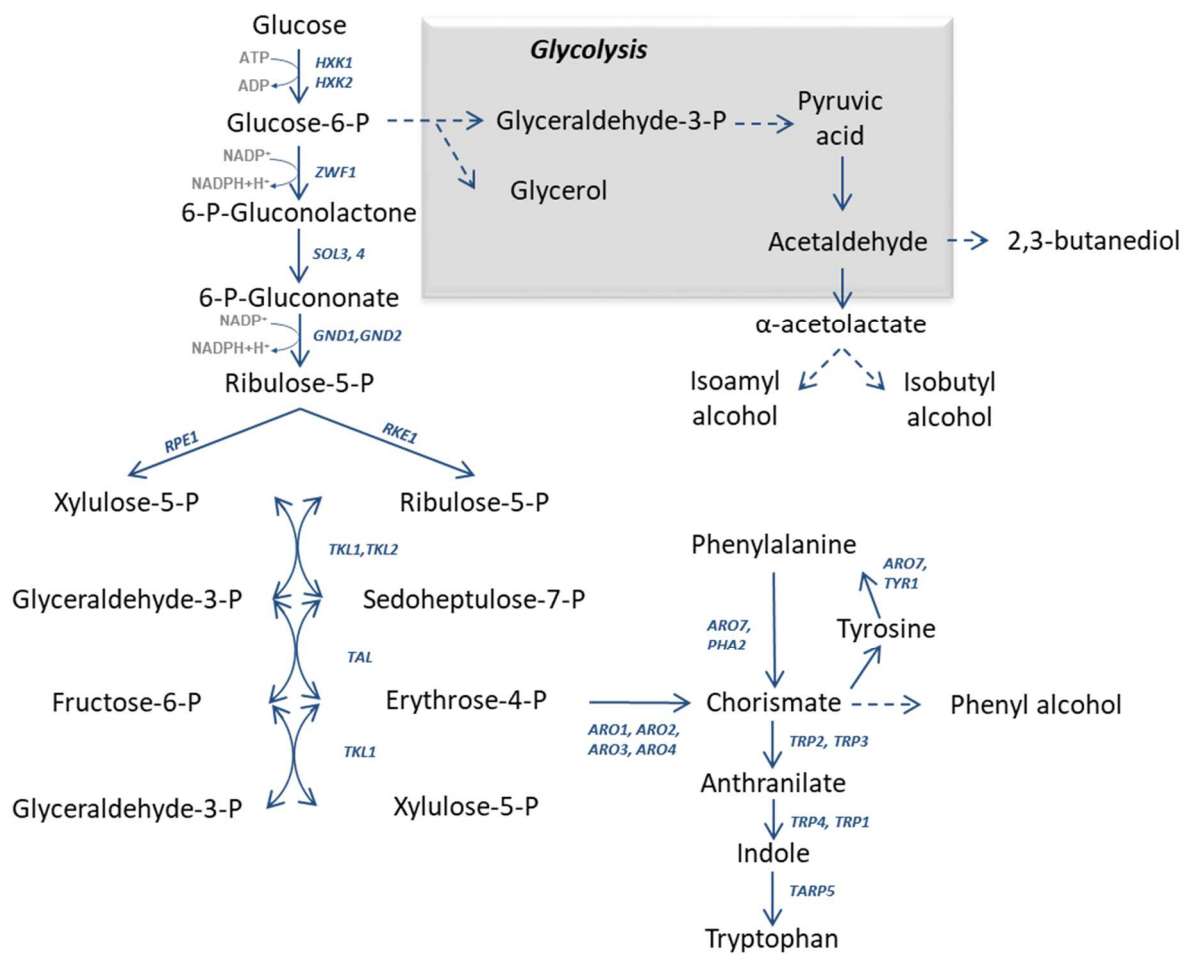
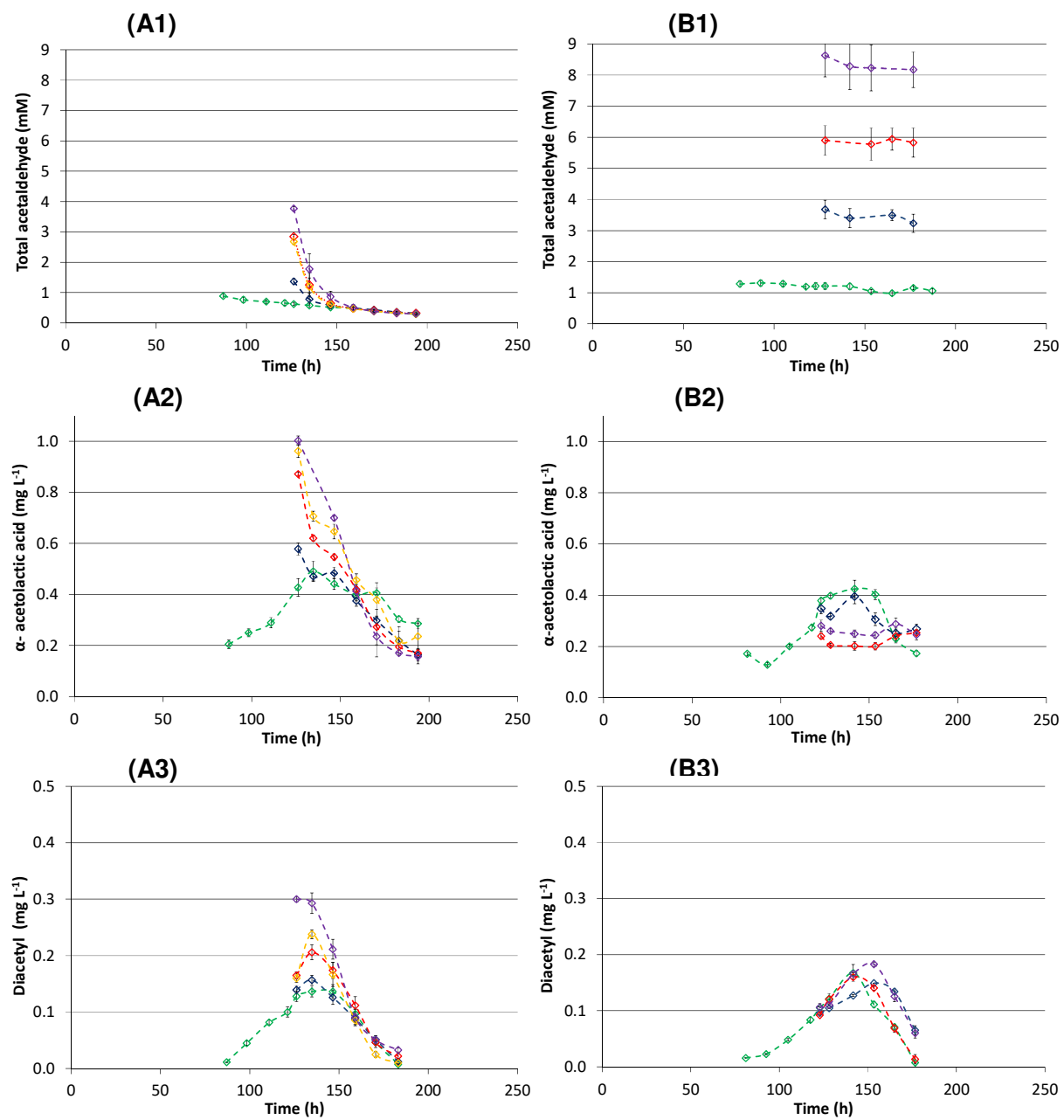


Figure 7.



Supplementary data

